Available online at www.sciencedirect.com
ScienceDirect
Polymer 47 (2006) 7189–7197
polymer
www.elsevier.com/locate/polymer

Molecular dynamics in semifluorinated side-chain polyesters as studied by broadband dielectric spectroscopy

Julius Tsuwi [a,*], Lutz Hartmann [a], Friedrich Kremer [a], Doris Pospiech [b], Dieter Jehnichen [b], Liane Häußler [b]

[a] *Institute for Experimental Physics I, University of Leipzig, Linnéstraße 5, 04103 Leipzig, Germany*
[b] *Leibniz-Institute of Polymer Research Dresden, Hohe Straße 6, 01069 Dresden, Germany*

Received 30 January 2006; received in revised form 18 April 2006; accepted 20 April 2006
Available online 23 June 2006

Abstract

The molecular dynamics in a variety of poly(ethylene isophthalate)s (PEIs) is studied by broadband dielectric spectroscopy (BDS). The materials comprise non-substituted main chain polyesters and polyesters with semifluorinated (oxydecylperfluorodecyl) side chains. Combining temperature-dependent small angle X-ray scattering (T-SAXS), differential scanning calorimetry (DSC) and BDS it can be shown that the microphase separated semifluorinated polymers exhibit independent dynamic glass transition relaxations taking place in the separate microphases. Additionally in the glassy state, the non-substituted polymers show an Arrhenius-type relaxation whose activation energy decreases gradually from 52 to 40 kJ/mol with increasing main chain flexibility. The semifluorinated polymers exhibit a relaxation assigned to fluctuations of the perpendicular component of the fluoroalkyl end group with activation energies between 38 and 40 kJ/mol. With increasing flexibility of the main chain, the dynamics of the backbone becomes faster for the non-substituted polymers while an opposite trend is observed in the oxydecylperfluorodecyl substituted side-chain materials. A detailed explanation of the molecular origin of the relaxations is provided.

Keywords: Dielectric spectroscopy; Molecular dynamics; Semifluorinated polymers

1. Introduction

Polymers with semifluorinated side chains have been investigated for about 15 years. The term ''semifluorinated'' here stands for chemical segments consisting of an alkyl- and a perfluorinated alkyl part, which are connected by a covalent C–C linkage, having the general structure $X_1-(CH_2)_n-(CF_2)_m-X_2$. Alkyl- and perfluoroalkyl chains are thermodynamically not miscible with each other. Therefore, such compounds are characterized by a strong microphase separation resulting in the formation of typically layer-like, well-organized solid-state structures [1,2]. If such semifluorinated segments are attached to polymeric backbones, the microphase separation of the semifluorinated segments can often be maintained assuming that the number of C-atoms in the semifluorinated (SF) segments (in both alkyl and perfluoroalkyl parts) is above a critical value. This is demonstrated for a set of polymers with varying polymer backbones and different semifluorinated side chains, for instance semifluorinated polystyrene [3], polystyrene–polyisoprene diblock copolymers [4], polymethylmethacrylate [5], polyesters [6–9], polysulfones [10], segmented polyester–polysulfone block copolymers [11,12] and others. In special cases where the semifluorinated side chains are long enough, the ordered solid-state results in the formation of a well-organized surface structure, resulting in polymeric materials with extremely low surface free energy [13–16]. Additionally, it turned out that the principal structural behaviour in the bulk and close to a surface is well comparable [14,15]. The structure formation in the surface layer depends not only on the chemical structure, but also on the film formation techniques (spin

* Corresponding author.
E-mail address: tsuwi@physik.uni-leipzig.de (J. Tsuwi).

0032-3861/$ - see front matter © 2006 Elsevier Ltd. All rights reserved.
doi:10.1016/j.polymer.2006.04.072

coating, dip coating, etc.) and the thermal history of the sample (annealing conditions, environmental conditions at storage, etc.). The results obtained until now were often not directly comparable because both the nature of the polymeric main chains as well as the detailed structure of the semifluorinated side chains were different. Thus, the complex interactions between main chains and side chains on the one hand and the properties in the bulk and close to a surface on the other hand could not completely be understood. Therefore, we started to use completely analogous semifluorinated side chains in order to obtain a comparison of the influence of semifluorinated side chains on the properties of the resulting polymer. Here, we would like to demonstrate the results for semifluorinated polyesters. We studied the thermal properties and the molecular dynamics of polyesters with systematic variation of the polymer backbone while keeping the semifluorinated side chains constant, thus comparing the influence of semifluorinated side chains on fully aromatic and semiaromatic polyester main chains. Long oxydecylperfluorodecyl segments [$-O-(CH_2)_{10}-(CF_2)_9-CF_3$] were chosen as semifluorinated side chains to have a strong driving force for microphase separation, as demonstrated before [6,9]. The principal chemical structure of the polymers investigated is outlined in Fig. 1 and the denotations of the investigated polymers are summarized in Table 1.

The fully aromatic polyester **1** and the semiaromatic polyesters **3**, **5** and **7** without any side chain were compared to polyesters with semifluorinated side chains (aromatic polyester **2** and semiaromatic polyesters **4**, **6** and **8**, respectively). The semifluorinated polymers contained constant semifluorinated (SF) side chains: $-O-(CH_2)_{10}-(CF_2)_9-CF_3$.

The comparison of polymers **2**, **4**, **6** and **8** having the same semifluorinated side chains allows us to evaluate the influence of the side chains on the backbone dynamics. Comparing polymers **1**, **3**, **5** and **7** enables us to study systematically the effect of main chain flexibility on the relaxational dynamics in the semifluorinated polymers. For that a combination of experimental tools like differential scanning calorimetry (DSC), temperature-dependent small angle X-ray scattering (T-SAXS) and broadband dielectric spectroscopy (BDS) is applied. The latter enables one to analyse separately fluctuations in the main chain and the side chain.

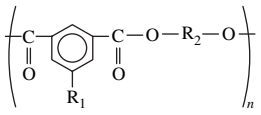

Fig. 1. General chemical structure of the polyesters investigated (where R_1 is $-H$ or $-O-(CH_2)_{10}-(CF_2)_9-CF_3$, and R_2 is $-Ph$ or $-(CH_2)_m$ with $m = 2$, 4 or 6. The chemical groups R_1 and R_2 and the denotations of the investigated polymers are summarized in Table 1.

Table 1
Chemical composition of the polymers investigated

Polymer	R_1	R_2
1	$-H$	$-Ph-$
2	$-O-(CH_2)_{10}-(CF_2)_9-CF_3$	$-Ph-$
3	$-H$	$-(CH_2)_2-$
4	$-O-(CH_2)_{10}-(CF_2)_9-CF_3$	$-(CH_2)_2-$
5	$-H$	$-(CH_2)_4-$
6	$-O-(CH_2)_{10}-(CF_2)_9-CF_3$	$-(CH_2)_4-$
7	$-H$	$-(CH_2)_6-$
8	$-O-(CH_2)_{10}-(CF_2)_9-CF_3$	$-(CH_2)_6-$

2. Experimental

2.1. Synthesis

All polymers under discussion were synthesized by transesterification polycondensation in the melt, using for the fully aromatic polymers **1**–**2** transacetylation polycondensation [6,8] and for the semiaromatic polymers **3**–**8** transesterification of dimethyl esters with the aliphatic diols [10,17]. The chemical characterization of the polymers used for the current investigation is summarized in Table 2.

2.2. Characterization methods

2.2.1. Viscosity measurements

Inherent viscosities as a measure for molar masses were determined by using an Ubbelohde viscometer at 25 °C, pentafluorophenol/chloroform (1/1 v/v) as solvent mixture and a polymer concentration of 0.5 grams per deciliter (g/dL).

2.2.2. SEC measurements

Size exclusion chromatography was carried out by a Knauer (Germany) apparatus using a mixture of pentafluorophenol/chloroform (1/2 v/v) as eluent, PL MiniMix D separation columns, and RI detection. Molar masses were calculated relative to narrowly distributed polystyrene standards.

2.2.3. X-ray scattering

Small angle X-ray measurements were carried out at the polymer beamline A2 at HASYLAB (DESY Hamburg). The linear detector was placed in order to measure the scattering intensity as a function of the scattering vector q ($=(4\pi/\lambda)\sin\theta = 2\pi/d$, where $\lambda = 0.15$ nm) from 0.2 to 2.85 nm^{-1} (with corresponding Bragg spacings from 30 to 2.2 nm, respectively). The samples had a thickness of about 0.5–1 mm and were wrapped into aluminium foil (with a thickness of 15 μm). The following temperature protocol was used: the samples were heated to 573 K with 3 K/min, held there for 5 min and subsequently cooled down to room temperature with the same rate.

Table 2
Chemical characterization of the polymers under investigation

Polymer	η_{inh} (g/dL)	$M_{n,SEC}$ (g/mol)	$M_{w,SEC}$ (g/mol)	M_w/M_n (–)
1	Not soluble in all solvents known for polyesters			
2	0.33	28,000	57,600	2.06
3	0.71	15,200	54,500	3.59
4	0.04	43,200	92,700	2.15
5	0.41	8750	18,500	2.12
6	0.19	Not detectable (isorefractive)		
7	0.39	11,600	24,900	2.15
8	0.39	Not detectable (isorefractive)		

Accumulation and waiting time were chosen so that temperature steps from frame to frame correspond to temperature intervals of 3 K.

2.2.4. DSC

DSC measurements were performed using a DSC-7 (Perkin Elmer) at a heating and cooling rate of 20 K/min. Glass transition temperatures were determined by the half-step method.

2.2.5. Broadband dielectric spectroscopy (BDS)

To prepare the samples, the materials were heated in vacuum until they melted and kept between two brass electrodes (diameter: 10 mm) with 50 μm glass fibre spacers. Isothermal dielectric measurements were performed in the frequency range from 0.1 Hz to 10 MHz using a High Resolution Dielectric Alpha-analyser (Novocontrol GmbH). Dielectric spectra were obtained starting from the highest temperature for the range 500–120 K in steps of 2 K. In this temperature range, the polymers were found to be thermally stable. The sample temperature was controlled by a gas heating system based on evaporation of liquid nitrogen (Quatro, Novocontrol GmbH) with a precision of ±0.02 K. Details of the set up are found elsewhere [18].

The dielectric loss ε'' was fitted to a superposition of a conductivity contribution with one or two relaxation functions according to Havriliak and Negami [19].

$$\varepsilon''(\omega) = \frac{\sigma_o}{\varepsilon_o}\frac{a}{\omega^s} + \mathrm{Im}\left[\frac{\Delta\varepsilon}{[1+(\mathrm{i}\omega\tau)^{\beta}]^{\gamma}}\right] \quad (1)$$

The first part on the right-hand side of the equation describes the conductivity while the second part (that is added) is the dipole contribution to the dielectric loss function. In this notation, one relaxation process is assumed. β and γ are dimensionless parameters describing the symmetric and asymmetric broadening of the distribution of relaxation times, respectively, with $0 < (\beta, \beta\gamma) \leq 1$. For $\beta = \gamma = 1$, Eq. (1) coincides with the ideal Debye-relaxation. ε_o is the permittivity of free space and σ_o is the direct current (d.c.) conductivity. The exponent s equals one for Ohmic behaviour while deviations ($s < 1$) are caused by electrode polarization or Maxwell–Wagner polarization effects (a is a factor having the dimensions $[\mathrm{Hz}]^{s-1}$ for $s \neq 1$). From the fits according to Eq. (1) the relaxation rate $1/\tau_{max}$ can be deduced which is given at the frequency of maximum dielectric loss ε'' for a given temperature. Within experimental uncertainty, Eq. (1) describes our data well. The term $\Delta\varepsilon$ is the relaxational strength, which can be used to estimate the value of the net dipole moment taking part in the relaxation process. This can be done through the Kirkwood–Fröhlich theory [20–23] from the relation

$$\Delta\varepsilon \approx n\frac{\mu^2}{3k_B T\varepsilon_o}g_{FK} \quad (2)$$

where g_{FK} represents the Kirkwood–Fröhlich dipole correlation factor, μ is the net dipole moment, n the dipole density, k_B is the Boltzmann constant, T is the absolute temperature and ε_o as explained in Eq. (1).

3. Results and discussion

3.1. Temperature-dependent SAXS

The solid-state structure of the investigated polymers with semifluorinated side chains shows similarities concerning their typical layered structure due to the non-compatibility of the backbone with the side chains. Earlier investigations [8,9] at room temperature and molecular modelling [7] confirm the expected intra-molecular phase separation with interdigitation of the side chains.

Fig. 2 shows a temperature-dependent small angle X-ray scattering contour plot of semifluorinated polymer **8** as an example for the substituted polyesters. From the figure, it can be observed that at room temperature the sample has stable layers ($d \sim 5.45$ nm). With increasing temperature, a slight increase in the d value is observed at about 82 °C followed by a general negative thermal expansion coefficient up to 151 °C where the layer structure collapses. Above 151 °C, no layer structures are observed. On cooling, layer formation is detected at 145 °C and the layer distance increases gradually reaching a stable d value of about 5.5 nm at 59 °C. The behaviour displayed by polymer **8** in Fig. 2 is representative of all the semifluorinated polymers investigated with slight differences in the temperature at which stable layers are formed and/or deformed. For purposes of this paper, it is sufficient to observe that the semifluorinated polymers investigated have stable layers at room temperature that disappear at elevated temperatures and reappear on cooling. This thermal characteristic is fully reversible.

3.2. Differential scanning calorimetry (DSC) of non-substituted samples

The thermal behaviour of the non-substituted main chain polyesters **3**, **5**, and **7** based on *m*-linked isophthalic acid and different diol spacers can be described by an amorphous structure (only glass transition detectable, see Fig. 3a). T_g shifts to lower temperatures with increasing length of the diol in the backbone. In contrast, the fully aromatic polymer **1** does not show any thermal transition over the entire temperature range of measurement (highly crystalline [24], no T_g in DSC visible, but expected to be ~150 °C [25] and weak effects in SAXS (compare Table 3)).

3.3. Differential scanning calorimetry (DSC) of semifluorinated samples

In Fig. 3b, the DSC curves of all the semifluorinated polymers **2**, **4**, **6** and **8** are presented. It can be observed from the figure that three main endothermic peaks exist. For purposes of clarity, the peaks are labeled *i*, *ii* and *iii* according to their order of occurrence from low to high temperature and using the fully aromatic polymer **2** as the reference. The assignment of the peaks has already been done earlier [8]: peak *i* (52 °C) corresponds to melting/crystallization (T_m) of the semifluorinated side chains, *ii* (130 °C) is the glass transition temperature (T_g) of the polymer backbone, and *iii* (198 °C)

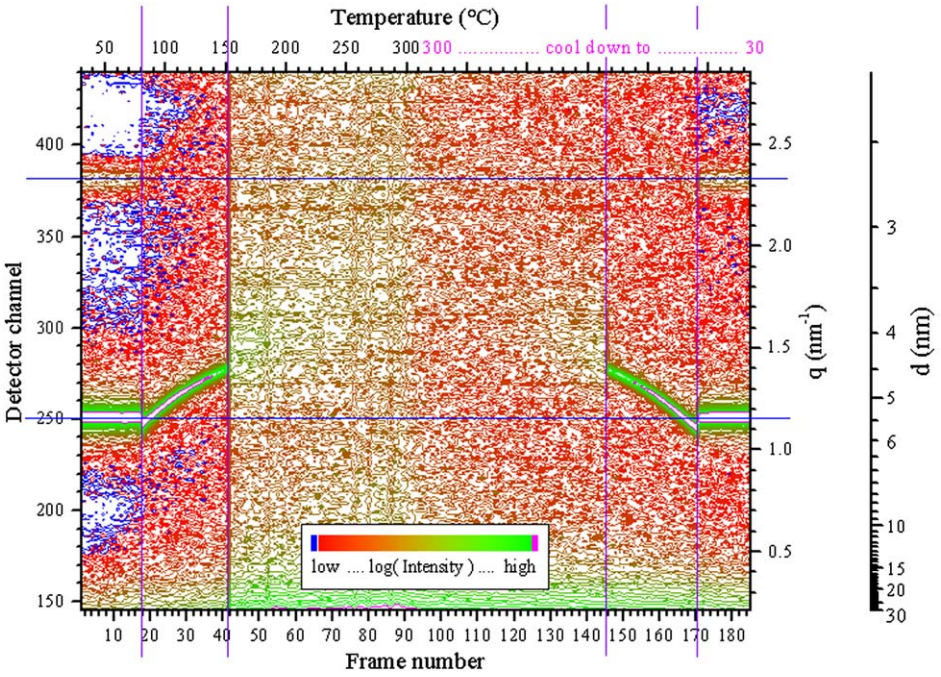

Fig. 2. Temperature-dependant SAXS contour plot of polymer **8** for both heating and cooling with 3 K/min in the temperature range 30–300 °C.

is the isotropization temperature (T_i), where the ordered layered structure disappears.

The transition temperatures of the investigated polymers as obtained by DSC and T-SAXS are shown in Table 3. From the comparison of thermal behaviour of the fully aromatic polymer **2** with the semiaromatic polymers **4**, **6** and **8** in Fig. 3b, three observations can be made. Firstly, T_g of the semiaromatic backbone is shifted to lower temperatures in **4** and not observable by DSC in **6** and **8**. Secondly, T_m of semifluorinated side chains occurs in the temperature range between 75 and 100 °C up from 52 °C with increased endothermic intensity. Thirdly, T_i is generally reduced in the semiaromatic polymers compared with polymer **2**.

3.4. Broadband dielectric spectroscopy (BDS)

Fig. 4 shows the frequency dependence of the dielectric loss ε'' for both the fully aromatic and semiaromatic non-substituted main chain polymers at different temperatures. Two relaxation processes, β and β* (according to the sequence of their mean relaxation times) are observed for the fully aromatic polyester (Fig. 4a). For the semiaromatic main chain polyester, an additional faster process, γ_B, is detected showing up as a shoulder on the high frequency wing of the β-process (Fig. 4b) at freezing temperatures. At elevated temperatures, the low frequency wing of the dielectric loss ε'' curve rises steadily due to conductivity contributions from mobile charge

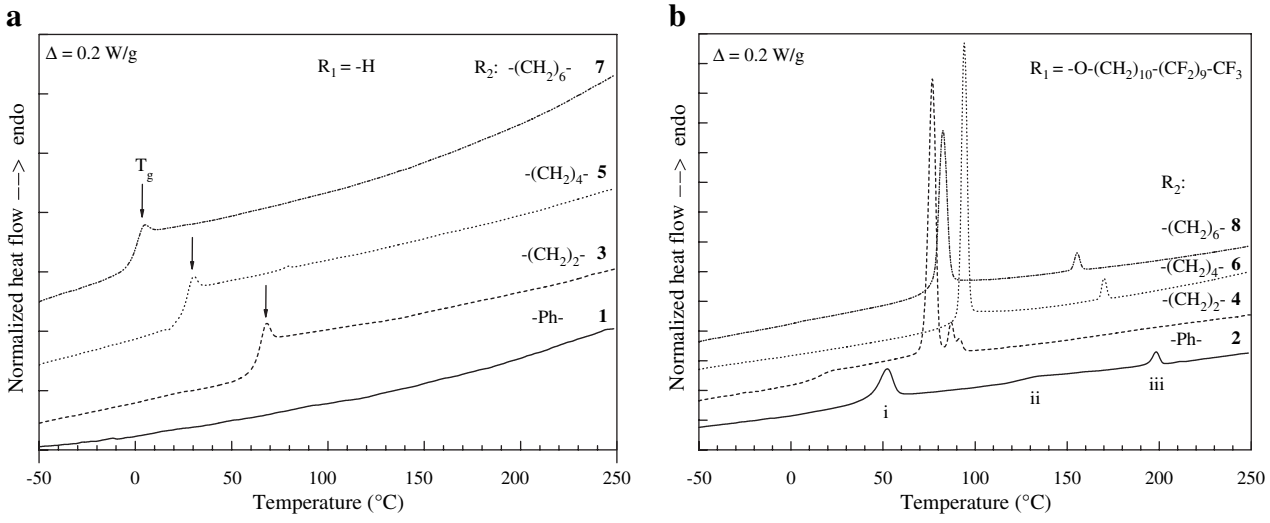

Fig. 3. DSC plots of the non-substituted (Fig. 3a) and the semifluorinated substituted side chain (Fig. 3b) polyesters under discussion. The numbers *i*, *ii* and *iii* in Fig. 3b represent the three thermal transitions as explained in the text.

Table 3
Summary of thermal transition temperatures of the non-substituted and the substituted polyesters as obtained by DSC (second Heating Run), temperature-dependant SAXS and broadband dielectric spectroscopy (BDS) measurements

Polymer	T_g (°C) DSC/T-SAXS[a]/BDS (α; δ)[b]	T_m (°C) DSC/T-SAXS/BDS	T_i (°C) DSC/T-SAXS/BDS	d (nm) (T-SAXS)[b]
1	–/∼165[c]; ∼265[d]; ∼325[e]/–	–/∼405/–	–	–
2	130[f]/110; 140/21.5; 85	52[f]/–/47.4	197[f]/–/–	4.65[g]
3	62.2/–/58.7	–	–	–
4	15.2/65/23.6; ∼40	77/75/67	86/–/–	5.60[g]
5	25/–/18.5	–	–	–
6	–/–/81.3; ∼40	94/–/87.5	170/–/–	5.65[g]
7	−3/–/−10	–	–	–
8	–/–/64.1; ∼40	83/82/75.2	155/145; 151/–	5.50[g]

T_g, T_m and T_i are the glass transition, melting and isotropization temperatures respectively. The layer distances d for the semifluorinated-substituted polymers are also included.

$\Delta T_{DSC} \approx \pm 0.1$ K; $\Delta T_{T\text{-}SAXS} \approx \pm 1.5 \ldots 2$ K.

[a] $\boldsymbol{T_{L1 \rightarrow L2}}$ – phase transition between different layer structures (corresponds to T_g).

[b] Only polymers **2**, **4**, **6** and **8** have δ-relaxations (from which by extrapolation to $1/\tau = 0.01$ a glass transition temperature could be deduced) from BDS and d values from T-SAXS.

[c] T_g, glass transition temperature.

[d] T_x (transition not known yet).

[e] lt → ht phase transition, taken from Ref. [24].

[f] See also Ref. [8]

[g] Taken from Ref. [17]

carriers. Additionally, electrode polarization or Maxwell–Wagner polarization effects can be seen. The temperature dependence of the dielectric loss of the semifluorinated substituted side-chain polyesters is shown in Fig. 5. From the figure two relaxations γ_{SF} and β below room temperature can be observed followed by melting of side chains between 315 and 365 K and finally the α and δ regions occur which are dominated by conductivity contributions. In the vicinity of the side chain melting, the α-process is hardly observable in the more flexible backbone polymers **6** and **8**. One more peculiar observation in Fig. 5 is the relaxation intensity of γ_{SF} and β. The fully aromatic polymer **2** has a higher γ_{SF}-relaxational strength when compared to the β-relaxation. The semiaromatic polymer **4** shows an opposite effect, while **6** and **8** having almost evened γ_{SF} and β intensities. It should be noted that γ_{SF} and β are relaxations originating from the semifluorinated side chain and the main chain (as will be shown later in the paper), respectively. By analysing them in detail together with the δ-relaxation, it is possible to elucidate the effect of the side chain on the molecular dynamics of the main chain and vice versa.

3.5. Influence of main chain flexibility on its relaxation behaviour

Fig. 6 shows the temperature dependence of the relaxation times of four samples (**1**, **3**, **5** and **7**) that differ in the structure of their main chains. It should be stated again here that the structure was varied by substituting R_2 (according to Fig. 1) with either phenyl ring (–Ph–) or $-(CH_2)_2-$, $-(CH_2)_4-$ or $-(CH_2)_6-$ diol groups. The β-process is observed in all the polymers, with the most flexible polymer **7** showing an additional γ_B-relaxation. An α-process is observed in **3**, **5** and **7** while polymer **1** shows a β*-relaxation instead.

3.6. The α-process

This is the dynamic glass transition process of the polymers. The data can well be described by the empirical Vogel–Fulcher–Tammann (VFT) [26] function as

$$\frac{1}{\tau} = \frac{1}{\tau_o} \exp\left[\frac{-DT_o}{T - T_o}\right] \tag{3}$$

where D is the fragility parameter [27], T_o is the Vogel temperature or the ideal glass transition temperature, τ is the relaxation time and τ_o ($=1/2\pi\nu_o$) is a preexponential factor. The calorimetric glass transition temperature (T_g) is conventionally defined as the temperature at which the relaxation time is 100 s [28]. By extrapolating the VFT dependence to logarithm $1/\tau_{max} = -2$, the T_g's of the compounds can be deduced. The values obtained for the semiaromatic polymers **3**, **5** and **7** are in agreement with DSC data within ±10 °C (see Fig. 3, Tables 3 and 4). The α-process becomes faster with increasing length of the aliphatic diol spacers due to the internal plasticization effect as observed in other polymeric systems [29,30]. The T_g of polymer **1** could not be estimated from the VFT fit because it presents a different kind of dynamics, which is separately discussed as a β*-process.

3.7. The β*-process

Polymer **1** is a rigid fully aromatic polyester that is highly crystalline [25] and hence does not show a glass transition (Fig. 3) in accordance with other studies [31–33]. The temperature dependence of its relaxation time τ can be described by the Arrhenius equation,

$$\frac{1}{\tau} = \frac{1}{\tau_o} \exp\left[\frac{-E_A}{RT}\right] \tag{4}$$

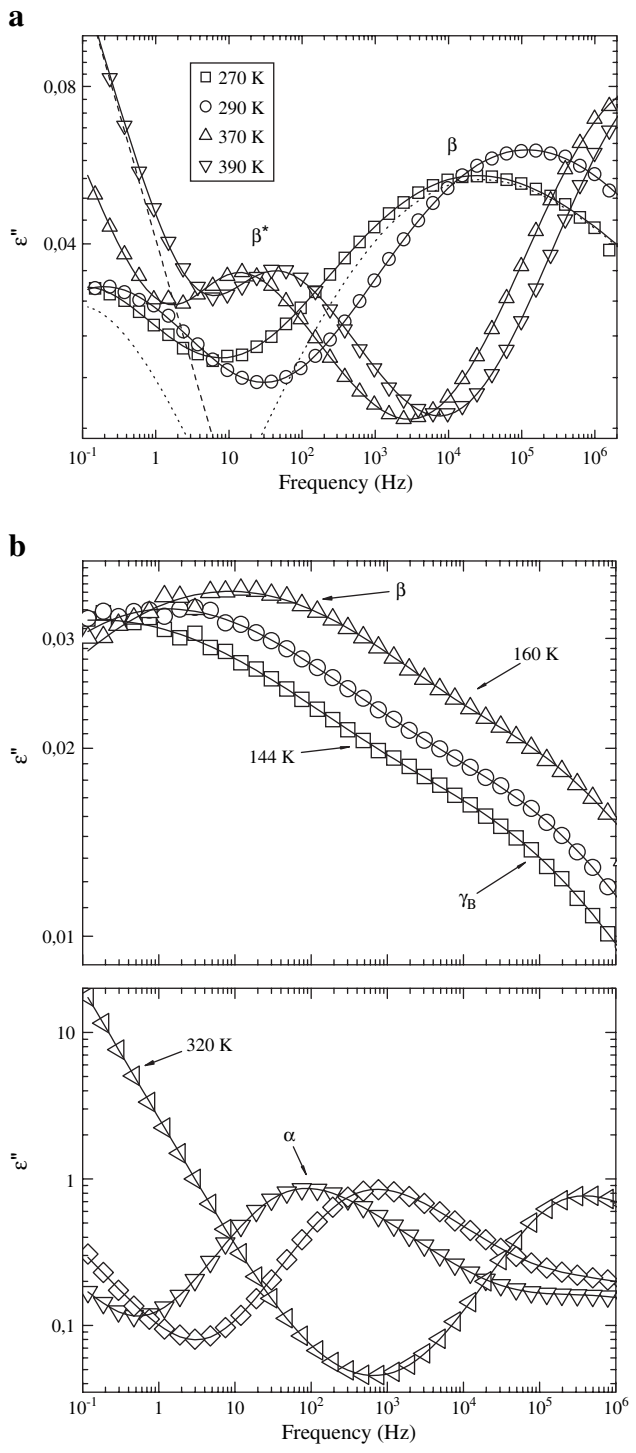

Fig. 4. (a) Dielectric loss ε'' versus frequency of the non-substituted basic aromatic polymer **1** at different temperatures as indicated. (b) Dielectric spectra for the semiaromatic polyester **7** at temperatures of 144 K (□), 150 K (○), 160 K (△), 284 K (▽), 290 K (◇) and 320 K (◁). Continuous lines (—) are fits according to Eq. (1) while dashed (– –) and dotted (····) lines indicate the separated conductivity and dipole fluctuation contributions, respectively.

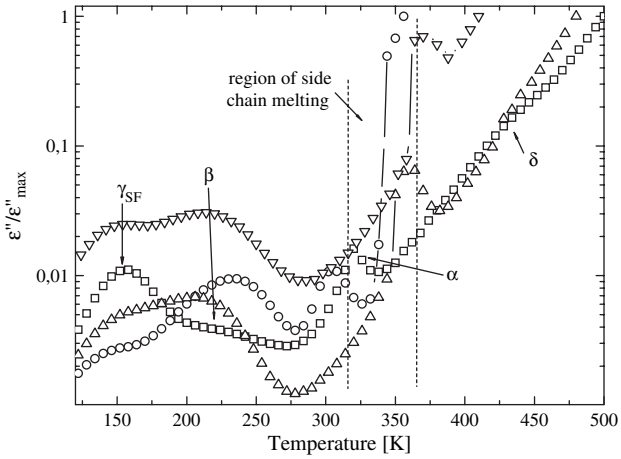

Fig. 5. Normalized dielectric loss ε'' versus temperature of the semifluorinated substituted side-chain aromatic polymer **2** (□) and the semiaromatic polymers **4** (○), **6** (△) and **8** (▽) at 970 Hz.

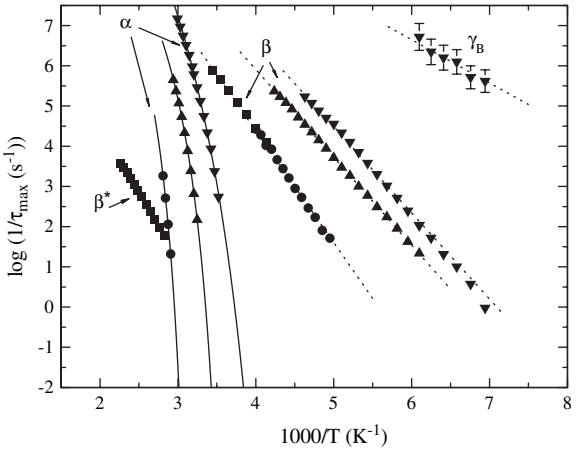

Fig. 6. Activation plot of the non-substituted main chain polyesters **1** (■), **3** (●), **5** (▲) and **7** (▼). The dotted lines indicate Arrhenius fits according to Eq. (4). Straight lines are VFT fits according to Eq. (3). Both Arrhenius and VFT fit parameters are shown in Table 4. Representative error bars are indicated; otherwise, error bars are smaller than the size of the symbols.

Table 4
Arrhenius and Vogel–Fulcher–Tammann (VFT) fit parameters of the non-substituted PEIs

Polymer	Arrhenius fit parameters				VFT fit parameters		
	γ_B-Relaxation		β-Relaxation		α-Relaxation (dynamic glass transition)		
	E_A (kJ/mol)	$\log(1/\tau_o)$ [τ_o (s)]	E_A (kJ/mol)	$\log(1/\tau_o)$ [τ_o (s)]	$\log(1/\tau_o)$ [τ_o (s)]	A ($=DT_o$) (K)	T_g (K)
1	–	–	52.8	15.5	–	–	–
3	–	–	52.8	15.5	10.9	197.8	331
5	–	–	41.8	14.6	11.3	205.5	291
7	20.5	13.1	41.0	15.2	14.5	412	260

with E_A denoting the activation energy and R is the universal gas constant. Its activation energy is 62 kJ/mol, similar to that obtained for the β-process in semicrystalline PET [31] and amorphous PEN [34]. It is assigned to fluctuations of carbonyl groups coupled with the phenyl rings [33]. Because the polymer is highly crystalline, the mobility of the carbonyl groups and the phenyl rings is presumably constrained hence it has a low dielectric strength $\left(\Delta\varepsilon_{\beta^*} \approx 0.09 \text{ at } 290\text{ K}\right)$.

3.8. The β-process

The β-relaxation is observed in all non-substituted polymers (Fig. 6). It has Arrhenius-type temperature dependence with activation energies between 41 and 53 kJ/mol (Table 4) and is assigned to fluctuations of the carbonyl groups which are adjacent to the phenyl rings. Flips of the latter have activation energies of about 0.5 eV [35] (=48.2 kJ/mol) thus supporting the above interpretation. In the high temperature limit, the β-relaxation has unrealistic high values for τ_o [36] (see Table 4). This is presumably caused by the fact that the coupling between phenyl rings and fluctuations of the carbonyl groups becomes weaker with increasing temperature. Hence a simple extrapolation of the β-relaxation rate to high temperatures is not justified. With increasing chain flexibility, the process becomes faster (see Fig. 6) owing to unrestricted motion of the carbonyl and the phenyl groups.

3.9. The γ_B-process

The γ_B-relaxation is observed only in polymer **7** with the most flexible R_2 group. The fact that it is observed in the sample with a six-fold aliphatic spacer and not in the others proves that the process originates from the substituted spacers that constitute R_2. It is also spacer length dependent. The Arrhenius-type temperature dependence relaxation rate with low activation energy ($\sim 20 \pm 5$ kJ/mol, see Table 4) and the weak dielectric strength ($\Delta\varepsilon < 0.05$) are characteristic of localized fluctuations [36]. This process is assigned to librational fluctuations of the alkoxy linker [37,38]. Since the aliphatic spacer itself is non-polar, its mobility can be dielectrically active only if some adjacent polar group is connected to it, for example an oxygen atom. It has been pointed out in side-chain liquid crystalline polymers [39–43] and related studies [44] that the process is observed for polymer systems with at least four spacer units. This agrees well with our observation that the γ_B-relaxation is only observed in polymer **7**, which has six $-CH_2-$ spacer units.

3.10. The effect of substituting semifluorinated side chains on the main chain relaxation

From the SAXS results, the semifluorinated polymers are microphase separated and have stable layers. Molecular dynamics in microphase separated systems is known to be characterized by independent motions in each microphase [29,45–47]. For our case, the backbone and the semifluorinated side chains form two microphases. It is therefore expected that each phase exhibits a separate glass transition process, which we denote as α and δ for the main chain and the perfluoroalkyl domains, respectively.

3.11. The α- and δ-processes

The α-relaxation is usually described as the motion of the polymer backbone segments [48]. For the non-substituted PEIs, it was found out that the calorimetric and dielectric T_g's were in good agreement. In microphase separated systems, a subtle interplay between the dynamics of the polymer backbone and the attached side groups characterizes the α-relaxation. The apparent glass transition temperatures of the backbone increase systematically with increasing flexibility (see Table 3 for the dielectrically determined glass transitions; α-relaxation. Polymer **6** shows higher values both for T_g, T_m and T_i. Work is currently going on in order to understand this exceptional case). A corresponding decrease in layer distance d (with the exception of **6**) for the semiaromatic polymers was also reported in an earlier publication [17]. This may be interpreted to mean that the flexible backbones attain favourable conformation in order to accommodate the rigid CF groups and hence results in smaller values of d. In turn, the aliphatic spacer groups (both from the side chain and from R_2) around the backbone slow the α-process. The non-substituted PEIs show the opposite trend. Polymer **4** in Fig. 7 shows a faster backbone motion before melting, interpreted as an earlier dynamic glass transition of the main chain due to the well segregated microphase. After melting of side chains, main chain fluctuation is slowed down and simultaneously the side chain undergoes its own glass transition, presented here as the δ-process. Thus we assign the δ-relaxation to the dynamic glass transition of the fluoroalkane domain in accord to our earlier work [29] and other studies [46]. The δ-process exhibits a temperature-dependent relaxation rate described by Eq. (3). The estimated T_g for the CF domain is about 40 °C for all the semiaromatic polymers and 85 °C for aromatic polymer **2**. For a maleimide backbone as that used in Ref. [29], the T_g for the CF domain was found (calculated from T_o values) in the range from 26 to 50 °C. This indicates that mobility of the CF domain depends on the flexibility of the main chain. The T_g's from DSC and the solid–solid transition(s) from T-SAXS may be considered to reflect motion of the CF microphase. For the flexible polymer **4**, the glass transitions of both domains are within close proximity thus only one T_g is detected in DSC. The highly flexible

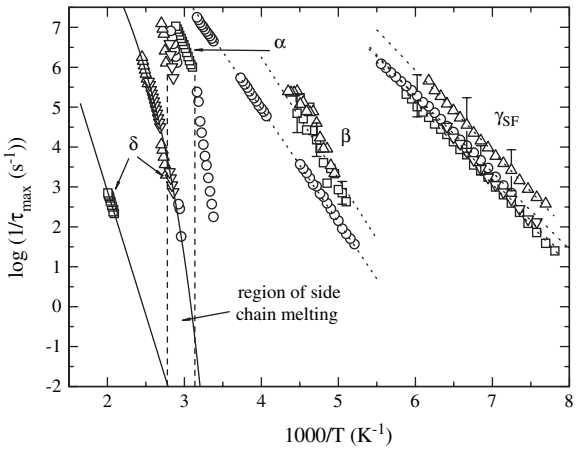

Fig. 7. Activation plot of the semifluorinated substituted side-chain polymers **2** (□), **4** (○), **6** (△) and **8** (▽). The dotted lines indicate Arrhenius fits according to Eq. (4), while straight lines are VFT fits according to Eq. (3). Dashed lines indicate the temperature range, within which melting of side chains occur. Representative error bars are indicated; otherwise, error bars are smaller than the size of the symbols.

polymer **8** shows no calorimetric T_g presumably because it takes place simultaneously with the side chain.

3.12. The β-process

With the CF units attached, the β-process generally becomes faster as shown in Fig. 7 (polymer **8** is not shown because there was no well-defined peak to realize good fits. See Fig. 5 instead). Polymers **2** and **6** have faster dynamics than **4**. The net dipole moment estimated from Eq. (2) gives 4.8 Debye ($1\ D = 3.336 \times 10^{-30}$ As m) for the rigid main chain polymer **2** and 18.4 D for both **4** and **6** at 220 K. The estimated dipole value for **4** and **6** is too high to be accounted for only by an ester group relaxation. The magnitude of the dipole moment of the ester group is in the range 1.65–1.80 D [49,50], which is closer to the estimated values of polymer **2** than for **4** and **6**. With the side chain attached at R_1, phenyl ring mobility is hindered. The main chain and the side chain for polymer **2** are both rigid and the bulk of the dielectric loss originates from dipole relaxation of the ester group. It is known that carbonyl (and so ester) group relaxation occurs at lower temperatures than phenyl ring motion [51]. Given that **4** and **6** have flexible main chain polymers, coupled carbonyl/phenyl dynamics is enhanced resulting in increased dielectric loss intensities (Fig. 5) and dielectric strengths.

3.13. The γ_{SF}-process

From Fig. 7 the γ_{SF}-relaxation is observed in all semifluorinated polymers unlike the γ_B-relaxation, which is only detected in polymer **7**. An Arrhenius fit gives activation energies between 38 and 40 kJ/mol which is higher than that obtained for the γ_B-process. The γ_{SF}-relaxation is two decades in frequency slower at 142 K than the γ_B-process. This indicates that the molecular origin of γ_{SF}- and γ_B-processes is not the same. The γ_{SF}-relaxation is assigned to librational motion of the perpendicular component of the fluoroalkyl end group in accordance to our previous work [29] and similar investigations [45,46].

The activation energy of γ_{SF}-relaxation is compared to other values in other fluorinated side-chain polymers: 31 kJ/mol [45] (with $-C_4F_9$ fluoroalkane unit on the side chain), 17 kJ/mol [46] ($-C_6F_{13}$), 30–36 kJ/mol [29] ($-C_7F_{15}$), 31 kJ/mol [45] ($-C_8F_{17}$), 36–37 kJ/mol [29] ($-C_9F_{19}$) and 38–40 kJ/mol ($-C_{10}F_{21}$) in this study. The polymers used in Refs. [29,45] have a linear backbone separated by different lengths of methyl spacers from the fluoroalkane side chain unit. A structure of ordered phase [52,53] was envisaged in analysing the results. By doubling the length of the fluoroalkane (CF) unit in Ref. [45], E_A was unchanged indicating that varying the length of CF unit does not affect E_A (within 10% uncertainty [29]). In Ref. [29], an activation energy of 33 ± 3 kJ/mol was obtained by varying the backbone structure (with constant spacer length of four units) and 35 ± 2 kJ/mol by changing the spacer length. The analysis of E_A for the different polymers with fluoroalkane side groups and different lengths of methyl spacers indicates that the dynamics of the γ_{SF}-relaxation is influenced by the type and flexibility of the backbone.

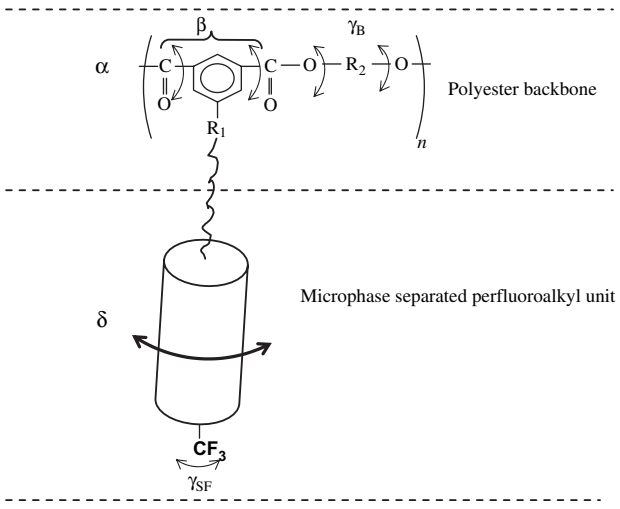

Scheme 1. Scheme to illustrate the different relaxation mechanisms discussed in the paper. The α- and δ-processes can be considered as independent glass transition processes of the backbone and the semifluorinated micro-domains, respectively. The fully aromatic main chain with no side chains (sample **1**) shows a β*-process instead because it's highly crystalline and hence does not have an α-process. β-relaxation is due to fluctuations of C=O groups. γ_B is a relaxation arising from the alkoxy substituents. γ_{SF}-relaxation is as a result of fluctuations at the terminal position of the fluoroalkyl unit.

4. Conclusions

Broadband dielectric spectroscopy has been employed to investigate the molecular dynamics in a variety of non-fluorinated and semifluorinated polyesters of subsequently varied molecular structure. The semiaromatic backbone exhibits an α-process which is assigned to the dynamic glass transition. For the highly crystalline backbone, a β*-process is observed instead. At lower temperatures two more processes β and γ_B occur, the former assigned to relaxation of the carbonyl group while the latter is obtained only after substituting one phenyl ring with diol groups. The semifluorinated side chains exhibit a δ-process assigned to a dynamic glass transition of the semifluorinated microphase. Additionally, an independent γ_{SF}-process is observed that is assigned to librational fluctuations of the perpendicular component of the fluoroalkyl end group. A scheme to illustrate the different relaxation mechanisms is provided (Scheme 1). The polymers studied are characterized by a strong thermal reversibility as seen from temperature-dependent SAXS data. The layered structure can be regarded as typical of microphase polymers. It has been found that by attaching the semifluorinated side chains, mobility of the main chain is enhanced. Introducing flexibility to the backbone of the semifluorinated materials has an opposite tendency to the plasticization effect found in the non-substituted polymers. This results in shifting the T_g of the polymer towards its melting temperature.

Acknowledgements

Financial support by the German academic exchange service (DAAD) for J. Tsuwi and German Science Foundation (grant number DFG Po 575/2-1, 2-2 and 7-1) is gratefully

acknowledged. The authors would like to thank Dr. S. Funari of the HASYLAB beamline A2 (DESY Hamburg), for providing measuring time and support during the temperature-dependant SAXS measurements. The support by Dr. H. Komber (NMR spectroscopy) and Mr. D. Voigt (SEC) (both IPF Dresden) for the chemical characterization of the polymers is gratefully acknowledged.

References

[1] Viney C, Russell TP, Depero LE, Twieg R. J Mol Cryst Liq Cryst 1989; 186:63.
[2] Viney C, Twieg RJ, Russell TP. J Mol Cryst Liq Cryst 1990;182B:291.
[3] Höpken J, Möller M. Macromolecules 1992;25:2482.
[4] Wang J, Mao G, Kramer EJ, Ober CK. Macromolecules 1997;30:1906.
[5] Chappell J, Lidzey DG. J Microsc 2003;209:188.
[6] Pospiech D, Jehnichen D, Häußler L, Voigt D, Grundke K, Ober CK, et al. Polym Prepr 1998;39:882.
[7] Friedel P, Pospiech D, Jehnichen D, Bergmann J, Ober CK. J Polym Sci Phys 2000;38:1617.
[8] Gottwald A, Pospiech D, Jehnichen D, Häußler L, Friedel P, Pionteck J, et al. Macromol Chem Phys 2002;203:854.
[9] Pospiech D, Jehnichen D, Gottwald A, Häußler L, Scheler U, Friedel P, et al. Polym Mater Sci Eng 2001;84:314.
[10] Pospiech D, Komber H, Voigt D, Jehnichen D, Häußler L, Gottwald A, et al. Macromol Symp 2003;199:173.
[11] Pospiech D, Häußler L, Eckstein K, Voigt D, Jehnichen D, Gottwald A, et al. Macromol Symp 2001;163:113.
[12] Grundke K, Pospiech D, Kollig W, Simon F, Janke A. Colloid Polym Sci 2001;279:727.
[13] Hyakawa T, Wang J, Xiang M, Li X, Ueda M, Ober CK, et al. Macromolecules 2000;33:8012.
[14] Pospiech D, Jehnichen D, Gottwald A, Häußler L, Kollig W, Grundke K, et al. Surf Coat Int Part B Coat Trans 2003;85:43.
[15] Jehnichen D, Pospiech D, Janke A, Friedel P, Häußler L, Gottwald A, et al. Mater Sci Forum 2001;378–381:378.
[16] Genzer J, Sivaniah E, Kramer EJ, Wang J, Xiang M, Char K, et al. Macromolecules 2000;33:6068.
[17] Pospiech D, Jehnichen D, Komber H, Voigt D, Häußler L, Friedel P, et al. Proceedings of IUPAC World Conference "Macro 2004", Paris; July 4–9, 2004.
[18] Kremer F, Schönhals A. Broadband dielectric spectroscopy. In: Kremer F, Schönhals A, editors. Berlin: Springer; 2003. p. 35 [chapter 2].
[19] Havriliak S, Negami S. Polymer 1967;8:161.
[20] Böttcher CJF. Theory of electric polarization. 2nd ed., vol. 1. Oxford: Elsevier; 1973. p. 181.
[21] Fröhlich H, Theory of dielectrics, Oxford; 1958.
[22] Onsager L. J Am Chem Soc 1936;58:1486.
[23] Kirkwood JG. J Chem Phys 1939;7:911.
[24] Jehnichen D, Friedel P, Bergmann J, Taut T, Tobisch J, Pospiech D. Polymer 1998;39:1095.
[25] Pospiech D, PhD thesis, ITP Dresden; 1989.
[26] Vogel H. Phys Z 1921;22:645; Fulcher GS. J Am Ceram Soc 1925;8:339; Tammann G, Hesse G. Z Anorg Allg Chem 1926;156:245.
[27] Angell CA. J Non-Cryst Solids 1991;131–133:13.
[28] Donth E. Glasübergang. Berlin: Akademie Verlag; 1981.
[29] Tsuwi J, Appelhans D, Zschoche S, Zhuang RC, Friedel P, Häußler L, et al. Colloid Polym Sci 2005;283:1321.
[30] Kremer F, Schönhals A. In: Kremer F, Schönhals A, editors. Broadband dielectric spectroscopy, vol. 1. Berlin: Springer; 2003. p. 400 [chapter 10].
[31] Boyd RH, Liu F. In: Runt JP, Fitzgerald JJ, editors. Dielectric spectroscopy of polymeric materials, Washington DC; 1997.
[32] Hardy L, Fritz A, Stevenson I, Boiteux G, Seytre G, Schönhals A. Polymer 2001;42:5679.
[33] Hardy L, Fritz A, Stevenson I, Boiteux G, Seytre G, Schönhals A. Polymer 2003;44:4311.
[34] Hardy L, Fritz A, Stevenson I, Boiteux G, Seytre G, Schönhals A. J Non-Cryst Solids 2002;305:174.
[35] Arrese-Igor S, Arbe A, Algería A, Colmenero J, Frick B. J Chem Phys 2004;120:423.
[36] Schönhals A. In: Kremer F, Schönhals A, editors. Broadband dielectric spectroscopy, vol. 1. Berlin: Springer; 2003. p. 243 [chapter 7].
[37] Groothues H, Kremer F, Pelsnivy T, Ringsdorf H. Macromol Chem Phys 1996;197:3881.
[38] Tsuwi J, Appelhans D, Zschoche S, Friedel P, Kremer F. Macromolecules 2004;37:6050.
[39] Zhong ZZ, Schule DE, Smith SW, Gordon WL. Macromolecules 1993;26:6403.
[40] Gedde UW, Liu F, Hult A, Sahlén F, Boyd RH. Polymer 1994;35:2056.
[41] Hellermark C, Gedde UW, Hult A, Boeffel C, Boyd RH, Liu F. Macromolecules 1998;31:4531.
[42] Zentel R, Strobl GR, Ringsdorf H. Macromolecules 1985;18:960.
[43] Borisova TI, Nikonorova NA. Macromol Chem Phys 1998;199:2147.
[44] Zhukov S, Stühn B, Borisova T, Barmatov E, Barmatova M, Shibaev V, et al. Macromolecules 2001;34:3615.
[45] Floudas G, Antonietti M, Förster S. J Chem Phys 2001;13:3447.
[46] Trahasch B, Stühn B, Lorenz K, Frey H. Macromolecules 1999;32: 1962.
[47] Volkov VV, Platé AN, Takahara A, Kajiyama T, Amaya N, Murata Y. Polymer 1992;33:1316.
[48] Schönhals A, Kremer F. In: Kremer F, Schönhals A, editors. Broadband dielectric spectroscopy, vol. 1. Berlin: Springer; 2003. p. 80 [chapter 3].
[49] Salz E, Hummel JP, Flory JP, Plavšić M. J Phys Chem 1981;85:3211.
[50] Krishna B, Bhargava SK, Prakash B. J Mol Struct 1971;8:195.
[51] Aoki Y, Brittain JO. J Appl Polym Sci 1976;20:2879.
[52] Shimizu T, Tanaka Y, Kutsumizu S, Yano S. Macromolecules 1996; 29:156.
[53] Lorenz K, Frey H, Stühn B, Mülhaupt R. Macromolecules 1997;30:6860.